



Magnetic Ground States of the Rare-Earth Tripod Kagome Lattice $\text{Mg}_2\text{RE}_3\text{Sb}_3\text{O}_{14}$ (RE = Gd, Dy, Er)

HPSTAR
306_2016

Z. L. Dun,¹ J. Trinh,² K. Li,^{3,4} M. Lee,^{5,6} K. W. Chen,⁶ R. Baumbach,⁶ Y. F. Hu,³ Y. X. Wang,³ E. S. Choi,⁶
B. S. Shastry,² A. P. Ramirez,² and H. D. Zhou^{1,6}

¹Department of Physics and Astronomy, University of Tennessee, Knoxville, Tennessee 37996-1200, USA

²Department of Physics, University of California, Santa Cruz, California 95064, USA

³Beijing National Laboratory for Molecular Sciences, State Key Laboratory of Rare Earth Materials Chemistry and Applications, College of Chemistry and Molecular Engineering, Peking University, Beijing 100871, People's Republic of China

⁴Center for High Pressure Science and Technology Advanced Research, Beijing 100094, People's Republic of China

⁵Department of Physics, Florida State University, Tallahassee, Florida 32306-3016, USA

⁶National High Magnetic Field Laboratory, Florida State University, Tallahassee, Florida 32310-3706, USA

(Received 8 January 2016; revised manuscript received 1 March 2016; published 12 April 2016)

We present the structural and magnetic properties of a new compound family, $\text{Mg}_2\text{RE}_3\text{Sb}_3\text{O}_{14}$ (RE = Gd, Dy, Er), with a hitherto unstudied frustrating lattice, the “tripod kagome” structure. Susceptibility (ac, dc) and specific heat exhibit features that are understood within a simple Luttinger-Tisza-type theory. For RE = Gd, we found long-ranged order (LRO) at 1.65 K, which is consistent with a 120° structure, demonstrating the importance of dipole interactions for this 2D Heisenberg system. For RE = Dy, LRO at 0.37 K is related to the “kagome spin ice” physics for a 2D system. This result shows that the tripod kagome structure accelerates the transition to LRO predicted for the related pyrochlore systems. For RE = Er, two transitions, at 80 mK and 2.1 K are observed, suggesting the importance of quantum fluctuations for this putative XY system.

DOI: 10.1103/PhysRevLett.116.157201

Introduction.—The two-dimensional kagome lattice magnet (KLM) has been a favorite in the theoretical condensed matter community since the experimental work on SCGO [1], due to the strong frustration associated with its network of corner-shared triangles. Many exotic states are predicted, such as the quantum spin liquid (QSL) state [2–4], the spin-orbital liquid state [5], the kagome spin ice (KSI) state [6], dipolar spin order [7], the Kosterlitz-Thouless (KT) transition [8], quantum order by disorder [9], nematicity, and supernematicity [10]. The large variety of exotic states predicted lies in contrast to a paucity of experimental systems. Early efforts include the exploration of langasites $\text{RE}_3\text{Ga}_5\text{SiO}_{14}$ [11–13], which possess distorted kagome lattices. Recent attention has been paid to vesignieite $\text{BaCu}_3\text{V}_2\text{O}_8(\text{OH})_2$ [14] and herbertsmithite $\text{ZnCu}_3(\text{OH})_6\text{Cl}_2$ [15]. The latter one shows intriguing signs of QSL behavior [15]. From a materials standpoint, however, these two systems are limited by (i) known defect-prone structures [14,16] and (ii) the inability to substitute facily on the magnetic site (e.g., with non-Heisenberg spins) to realize states other than the QSL. Clearly then, finding new KLM-containing compounds with spin-type variability is a challenge of the highest order.

Intriguingly, a 2D KLM is naturally contained in the frustrated 3D pyrochlore structure. In pyrochlores $\text{RE}_2\text{X}_2\text{O}_7$ (RE = rare-earth element, X = transition metal element), both the RE^{3+} and X^{4+} sublattices form alternating kagome and triangular layers along the [111] axis as a result of

corner-shared tetrahedrons [Fig. 1(a)] [17]. However, the strong interlayer interaction enforces three dimensionality. An exception is found in studies of $\text{Dy}_2\text{Ti}_2\text{O}_7$ in a [111] magnetic field, which polarizes the triangular layer spins,

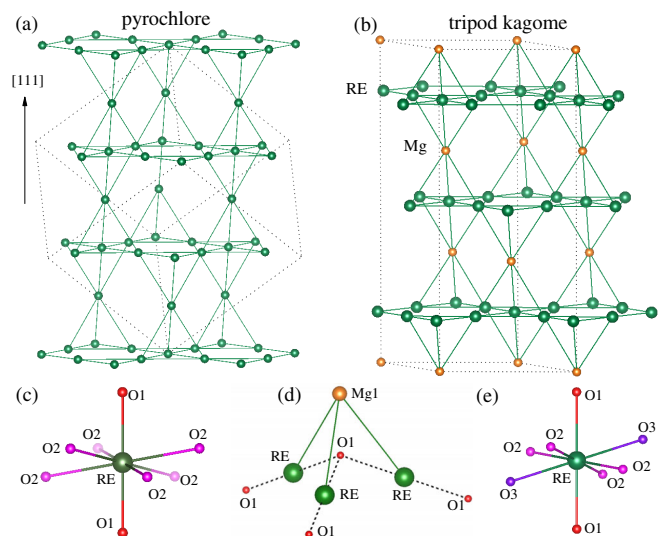


FIG. 1. (a) Alternating kagome and triangular layers in a pyrochlore lattice. (b) Alternating RE-kagome and Mg-triangular layers in a TKL. Dashed lines indicate a single unit cell. Local oxygen environments around RE^{3+} for (c) pyrochlore and (e) TKL. (d) A single “tripod.” Dashed lines represent Ising axes.

effectively decoupling the kagome planes, leading to a KSI state [17].

Obviously, if one can remove the magnetic moment of the triangular layers in the pyrochlore lattice, a RE-kagome-only lattice might be realized, enabling the study of intrinsic kagome physics. Because of various spin and spin anisotropies of different RE^{3+} ions, exotic and rich magnetic properties should be immediately available via the complex interplay among the spin-orbital coupling, dipolar and exchange interactions. In pyrochlores, for example, this interplay leads to multi- k ordering [18] with multiple field-induced transitions [19] for Heisenberg spins in $\text{Gd}_2\text{Ti}_2\text{O}_7$, spin ice state [20] for Ising spins in $\text{Ho}_2\text{Ti}_2\text{O}_7$ [21] and $\text{Dy}_2\text{Ti}_2\text{O}_7$ [22], and quantum order by disorder physics in the XY spin system $\text{Er}_2\text{Ti}_2\text{O}_7$ [23]. Then, what will be the magnetic ground states in the RE-based KLMs?

In this Letter, we have created such a KLM: $\text{Mg}_2\text{RE}_3\text{Sb}_3\text{O}_{14}$ based on partial ion substitution in the pyrochlore lattice. Here, the triangular layers in the pyrochlore structure are occupied by nonmagnetic Mg^{2+} ions, leaving the RE^{3+} -kagome layer well isolated from neighboring layers. We studied three representative systems ($\text{RE} = \text{Gd}, \text{Dy}, \text{Er}$) by dc and ac susceptibility ($\chi_{\text{dc}}, \chi_{\text{ac}}$) and specific heat [$C(T)$] measurements. We present a spin Hamiltonian and show the fundamental differences in collective behavior between the 2D KLMs and their 3D pyrochlore cousins.

Structure.—Sample synthesis method and measurement setups are described in the Supplemental Material [24]. $\text{Mg}_2\text{RE}_3\text{Sb}_3\text{O}_{14}$ ($\text{RE} = \text{Gd}, \text{Dy}, \text{Er}$) has a rhombohedral structure with R-3m space group. Compared with the pyrochlore lattice, the triangular layers of both RE^{3+} and Sb^{5+} sublattices in the KLM structure are occupied by Mg^{2+} (the Mg^{2+} site can be replaced by Co^{2+} [28], Mn^{2+} [29], Zn^{2+} [30]). Thus, the chemical formula can also be written as $(\text{Mg}_{0.25}\text{RE}_{0.75})_2(\text{Mg}_{0.25}\text{Sb}_{0.75})_2\text{O}_7$, which is a pyrochlore ($\text{RE}_2\text{X}_2\text{O}_7$) with 1/4 RE^{3+} and X^{4+} ions substituted in an ordered manner [Fig. 1(b)]. It is noteworthy that for the x-ray diffraction pattern of $\text{Mg}_2\text{RE}_3\text{Sb}_3\text{O}_{14}$ [24], the strongest peak for pyrochlore at $2\theta \sim 30^\circ$ disappears completely and splits into two peaks, providing evidence for the absence of Mg-RE or Mg-Sb site disorder [29]. As shown below, the $C(T)$ peaks at their phase transitions are very sharp, further underscoring the high degree of site order in the kagome layers. This good kagome layer separation is likely due to the large ion size difference between Mg^{2+} and RE^{3+} . In this structure, the nearest-neighbor distance between the RE^{3+} ions within a kagome layer remains similar to that of its pyrochlore cousin, and the RE^{3+} -kagome layers are well isolated from each other by the nonmagnetic Mg^{2+} , Sb^{5+} layers. Take $\text{Mg}_2\text{Gd}_3\text{Sb}_3\text{O}_{14}$, for example. The nearest Gd-Gd distance within a kagome layer (3.678 Å) is similar to that in $\text{Gd}_2\text{Ti}_2\text{O}_7$ (3.600 Å), and much smaller than that between different planes (6.162 Å). Since the

dipolar energy goes as $1/r^3$, this leads to interlayer energies an order of magnitude smaller than intralayer energies. Thus, the kagome lattice in $\text{Mg}_2\text{RE}_3\text{Sb}_3\text{O}_{14}$ is seemingly free of structural defects.

In pyrochlore $\text{RE}_2\text{X}_2\text{O}_7$, one important structural feature is that each RE^{3+} ion is surrounded by eight oxygens [Fig. 1(c)] with two shorter RE-O1 bonds lying along the local-[111] axis and six longer RE-O2 bonds forming a puckered ring. This feature defines the crystal electric field (CEF) and the g factor, which determines the ionic anisotropy for the RE^{3+} spins. In $\text{Mg}_2\text{RE}_3\text{Sb}_3\text{O}_{14}$, this local oxygen coordination is largely preserved. The RE ion is still surrounded by eight oxygens with the two shortest RE-O1 bonds that remain lying along the local-[111] axis [Fig. 1(e)]. The difference is that the longer six RE-O bonds are divided into two sets: four longest RE-O2 bonds and two intermediate RE-O3 bonds [24]. Since the CEF degeneracy has already been lifted by the pyrochlore-like anisotropy for an effective spin-1/2 system, the dominant anisotropy remains the one distinguishing the puckered ring from the local-[111] oxygens, making this in-plane anisotropy most likely irrelevant for the ground state degeneracy.

Given the high degree of site order, the large difference in separation between intraplane and interplane RE ions, it is appropriate to consider this a well-formed kagome structure. In addition, the CEF-driven single ion anisotropy, which is vestigial from the parent pyrochlore structure, defines directions for either the Ising spins or the XY -spin normal vectors that are neither uniaxial nor uniplanar. This particular situation of three distinct axes with specific interaxes angles will be important for understanding ordered spin configurations, as we show below. Given the uniqueness of this structure and the need to distinguish it from KLMs with undefined local anisotropy, we call this the “tripod kagome lattice” (TKL), inspired by a “tripod” formed by three RE^{3+} and one Mg^{2+} ion [Fig. 1(d)].

Magnetic properties.—For $\text{Mg}_2\text{Gd}_3\text{Sb}_3\text{O}_{14}$, a Curie-Weiss (CW) fit from 50–300 K of $1/\chi_{\text{dc}}$ [Fig. 2(a)] yields a Weiss temperature, $\theta_W = -7.35$ K, and an effective magnetic moment, $\mu_{\text{eff}} = 7.91 \mu_B$. The negative θ_W is close to that of $\text{Gd}_2\text{Ti}_2\text{O}_7$ ($\theta_W = -11.7$ K) [31]. The μ_B value is consistent with $\mu_{\text{eff}} = 7.94 \mu_B$ expected for Gd^{3+} ($^8S_{7/2}$). With measurement frequencies ranging from 80 to 700 Hz, χ_{ac} shows a sharp and frequency-independent peak at $T_N = 1.65$ K [Fig. 2(b)], indicating a long-ranged order (LRO) transition. This transition is further confirmed by a sharp peak at the same temperature in magnetic specific heat $C_{\text{mag}}(T)$ [Fig. 2(c)]. The magnetic entropy below 6 K is 17.16 J/(mol Gd) K [24]. This value is close to $R \ln(2S + 1) = 17.29$ J/mol K for a $S = 7/2$, indicating a complete LRO among the Gd^{3+} spins.

For $\text{Mg}_2\text{Dy}_3\text{Sb}_3\text{O}_{14}$, the CW fit below 10 K yields $\theta_W = -0.18$ K and $\mu_{\text{eff}} = 10.20 \mu_B$ [Fig. 2(d)], consistent with the free ion moment of $10.63 \mu_B$ for Dy^{3+} ($^6H_{15/2}$).

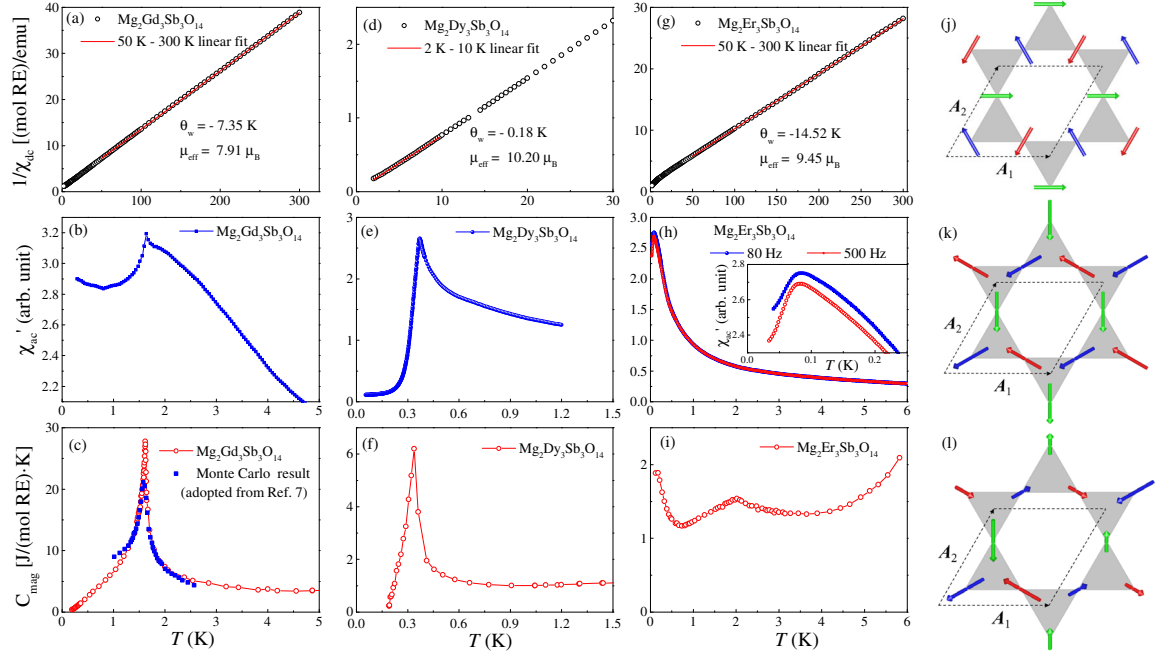


FIG. 2. (a)–(i) Temperature dependence of the inverse χ_{dc} , real part of the χ_{ac} , and magnetic specific heat C_{mag} for $Mg_2RE_3Sb_3O_{14}$. The blue dot in (c) is the Monte Carlo simulation result adopted from Ref. [7] with scaling. (j) The 120° LRO state for $Mg_2Gd_3Sb_3O_{14}$ and $Mg_2Er_3Sb_3O_{14}$. The dashed lines represent a unit cell. (k) The $k = 0$ LRO state and (l) the $k = (1/3, 2/3)$ spin-density-wave-like state for $Mg_2Dy_3Sb_3O_{14}$.

In $Dy_2Ti_2O_7$ [31], the small θ_W (-0.20 K) is due to competition between the dipolar interaction and superexchange couplings of Dy ions. Here, the similarity in local structure translates into similar-size coupling to the pyrochlore case, since the total spin-spin coupling is dominated by the dipolar interaction. With the ferromagnetic dipolar interaction, the negative θ_W again shows the antiferromagnetic nature of the exchange interactions in $Mg_2Dy_3Sb_3O_{14}$. A transition to LRO at $T_N = 0.37$ K is observed in both the χ_{ac} [Fig. 2(e)] and $C_{mag}(T)$ [Fig. 2(f)]. The integrated magnetic entropy below 6 K is 5.38 J/(mol Dy) K [24], which is close to $R \ln 2 = 5.76$ J/(mol Dy) K, as expected for a Kramers doublet. This suggests that the Dy^{3+} spins fully order below 0.37 K.

For $Mg_2Er_3Sb_3O_{14}$, the CW fit above 50 K yields $\theta_W = -14.25$ K, and $\mu_{eff} = 9.45 \mu_B$ [Fig. 2(g)], consistent with the free ion moment of $\mu = 9.58 \mu_B$ for Er^{3+} ($^4I_{15/2}$). The value for θ_W is close to that of the pyrochlore $Er_2Ti_2O_7$ ($\theta_W = -15.93$ K [31]). The χ_{ac} was measured down to 30 mK with a broad peak observed around 80 mK [Fig. 2(h)], which shows weak frequency dependence. The $C_{mag}(T)$ was measured down to 120 mK and exhibits a weak and broad peak around 2 K [Fig. 2(i)]. At this temperature, no anomaly is observed in χ_{ac} , while an extremely weak anomaly [2×10^{-8} emu/(mol Er)] was seen in χ_{dc} at 2.1 K, which is perhaps related to the weak $C_{mag}(T)$ peak.

Theoretical investigation and discussion.—The three systems discussed here, Gd, Dy, Er, are likely

representatives of the three different spin types, Heisenberg, Ising, and XY, respectively, evidenced by similar low temperature magnetization curves compared with their pyrochlore cousins [24]. In the pyrochlore systems discussed above, each spin type yields significantly different behavior. To uncover the possible differences among the spin types in the TKLs, we have used a Luttinger-Tisza-type theory [32,33] and studied the eigenvalues and eigenfunctions of the interaction matrix in wave vector space. We construct a 2D kagome lattice with \mathbf{A}_1 and \mathbf{A}_2 as basis vectors of the triangular Bravais lattice where there are three basis sites in a unit cell, labeled as blue, red, and green [Fig. 2(j)]. Thus, the general Hamiltonian for the TKL can be written as [24]

$$H = \frac{1}{2} \sum_{k, \alpha, \beta, a, b} S^{\alpha, a}(k) S^{\beta, b}(-k) V_{ab}^{\alpha\beta}(k), \quad (1)$$

where V is the sum of a dipolar part, exchange part, and a single ion anisotropy part dictated by the CEF effects. Here, α and β are the Cartesian indices of the spins and a, b run over the three basis sites in unit cell. The spin vector is the Fourier component of the real space object, and k runs over the Brillouin zone of the triangular lattice. Thus, for a given value of k , V is a 9×9 matrix that can be easily diagonalized. The dipolar part (D_{mn}) is fixed exactly by the effective moment of spin and RE-RE distances, while the exchange (J_{ex}) and single ion terms are found from the θ_W and the CEF splitting of the RE^{3+} in the given environment [24].

The $\text{Mg}_2\text{Gd}_3\text{Sb}_3\text{O}_{14}$ has Heisenberg spins ($J = 7/2$, $L = 0$) and therefore no single ion term. The θ_W of -7.35 K leads to an estimate of the exchange constant $J_{\text{ex}} \sim 6.10$ K, while the dipolar energy scale of nearest-neighbor spins $D_{\text{nn}} \sim 0.79$ K [24]. We found that the minimum eigenvalue of V is at the Brillouin zone (BZ) center with $k = 0$, and the corresponding eigenvector represents a 120° state where the three spins in the unit cell lie in the plane pointing along three axes at angles $2\pi/3$ to each other [Fig. 2(j)]. Here, the large dipolar term breaks the rotation invariance, lifts the frustration of a kagome lattice, and helps defeat the Mermin-Wagner theorem for a 2D Heisenberg lattice. It is known that higher values of spin than $1/2$ releases the frustration somewhat like soft spins would [34], and the case here has $S = 7/2$. This seems to enable a 2D-Ising-like transition with a logarithmic heat capacity in the style of Onsager. Actually, similar spin structure was predicted by Maksymenko *et al.* by considering classical dipoles on a kagome lattice [7]. Their calculated specific heat agrees well with our experiment in the critical region by proper scaling [Fig. 2(c)]. Thus, we conclude $\text{Mg}_2\text{Gd}_3\text{Sb}_3\text{O}_{14}$ to be a rare example of dipolar interaction mandated spin ordering on a kagome lattice.

The Dy^{3+} ion is an effective spin-1/2 Kramers ion with Ising anisotropy in an eight-oxygen-surrounding environment. Similar to the spin ice system, the Ising axis in the $\text{Mg}_2\text{Dy}_3\text{Sb}_3\text{O}_{14}$ variant is along the lines joining each Dy to O1 [dashed lines in Fig. 1(d)]. For the three sites in our Bravais lattice, the Ising directions are $\vec{n}_{\text{blue}} = \frac{1}{\sqrt{5}}\{\sqrt{3}, 1, 1\}$, $\vec{n}_{\text{red}} = \frac{1}{\sqrt{5}}\{-\sqrt{3}, 1, 1\}$, $\vec{n}_{\text{green}} = \frac{1}{\sqrt{5}}\{0, -2, 1\}$ in the global Cartesian frame. The small θ_W of -0.18 K corresponds to $J_{\text{ex}} \sim 1.12$ K, while the dipolar energy scale $D_{\text{nn}} \sim 1.31$ K [24]. It is known that ferromagnetic spins with tripodlike anisotropy on a kagome lattice are highly frustrated, which will lead to the KSI state [6]. Similar to that of the pyrochlore spin ice [20,22], the ice rule (spins with either two-in–one-out or one-in–two-out with respect to the center of each triangle) of KSI will also result in a large number of ground state degeneracy and zero-point entropy [6].

With the TKL and strong dipolar interaction, it is tempting to view $\text{Mg}_2\text{Dy}_3\text{Sb}_3\text{O}_{14}$ as a realization of a dipolar ferromagnet where the KSI physics could be realized. Our Luttinger-Tisza method yields a metastable state at the BZ center, which is an ordered KSI state. The corresponding spin structure [Fig. 2(k)] can be viewed as a three-sublattices ferromagnetic order with $k = 0$. This spin structure also resembles the theoretically predicted LRO state [35–37] for the 3D pyrochlore spin ice observed in $\text{Tb}_2\text{Sn}_2\text{O}_7$ [38]. However, this $k = 0$ state is *not* a global ground state. The lowest eigenvalue of the exchange matrix is found to be at the six K points of BZ corners, whose energy is somewhat lower than that of the zone center. Such an eigenvalue corresponds to a LRO state with a 3×3 tripled magnetic unit cell. In addition, the magnitude of the moment

differs in space, as prescribed by a commensurate spin density wave state. Unlike the $k = 0$ state where the KSI ice rule is preserved for every Mg-Dy tetrahedron [gray triangle in Fig. 2(k)], here, one out of six tetrahedrons violates the local ice rule. Note that the Luttinger-Tisza method used here is more akin to the mean-field theory when applied away from the zone center or the M point of the BZ. This is a nontrivial and complex problem (see, e.g., Refs. [39,40]) and requires further theoretical investigation. Regardless of the exact nature of ordering, our TKL system then appears to enable the spin dynamics to be much more efficient, as compared to the 3D $\text{Dy}_2\text{Ti}_2\text{O}_7$ compound. This interesting contrast therefore provides a strong impetus to the study of the underlying dynamics. Along with the observed LRO at 0.37 K, the Dy-Ising TKL provides a rare example exhibiting a LRO state that breaks the KSI degeneracy.

The Er^{3+} ion in $\text{Mg}_2\text{Er}_3\text{Sb}_3\text{O}_{14}$ has a large angular momentum $J = 15/2$. At low temperatures, it reduces to an effective spin-1/2 as a result of the Kramers doublet. The high temperature $\theta_W \sim -14.52$ K implies a large exchange energy $J_{\text{ex}} \sim 11.0$ K, while the dipolar energy scale is $D_{\text{nn}} \sim 0.11$ K by assuming a moment of $3 \mu_B$ [24] (similar to that in the Er pyrochlore). This implies that below ~ 10 K the spins are locked up into the state preferred by the exchange. The CEF in this case gives rise to a local XY model, where the Er^{3+} are energetically favorable to lie in the local XY plane perpendicular to the Ising axis discussed above. In the Er pyrochlore, such an XY model will give rise to a U(1) degeneracy in the spin Hamiltonian at the mean-field level that allows the Er^{3+} spins to rotate continuously in the XY plane [23]. In Er TKL, similar XY degeneracy is preserved for the exchange part of the Hamiltonian. However, an arbitrarily small long-range dipolar interaction will break the degeneracy. By diagonalizing the interacting matrix, a lowest energy eigenvalue is found at the BZ center whose eigenvector, by a curious coincidence, corresponds to the coplanar model exactly the same as that of the Gd compound [Fig. 2(j)].

Regarding the experimental observations for the Er TKL, since the 2.1 K anomaly in $C(T)$ is extremely weak in terms of the entropy under the peak, and χ_{dc} shows a similarly weak anomaly, the order parameter might be one that still allows significant fluctuations below its T_C , reminiscent of a KT transition [41] where spin vortices form and bind. Then the 80 mK transition shown on χ_{ac} is likely related to the predicted 120° coplanar antiferromagnetic ordering. If so, such a low ordering temperature (frustration index $f = (\theta_W/T_N) \sim 180$) suggests the importance of quantum spin fluctuations in terms of suppressing the ordering temperature and selecting the ordered state. The weak frequency dependence on χ_{ac} around the peak might indicate an increasing spin lattice relaxation time as temperature is decreased. The importance of thermal coupling between a coherent spin system and the lattice needs to be understood for both identifying and potentially using quantum materials

[42]. Future experiments including neutron scattering and muon spin spectroscopy will be useful to identify the nature of the two transitions at 80 mK and 2.1 K.

Summary.—We discovered a new 2D rare-earth TKL $\text{Mg}_2\text{RE}_3\text{Sb}_3\text{O}_{14}$ by partially substituting the ions in the cubic pyrochlore lattice. Our studies on three samples with $\text{RE} = \text{Gd}, \text{Dy}, \text{Er}$ have already related their magnetism to various exotic states including the dipolar spin order, the KSI, and the KT transition. Because of the large variability of the spin sets in the rare-earth family and the possibility of tuning the lattice parameters via chemical pressures, other exotic physics might also be realized. Future exploration of the whole TKL family members is expected to open a new field in condensed matter physics and materials science studies for coming years, such as the pyrochlore did during the past two decades.

The work of B. S. S. at UCSC was supported by the U.S. Department of Energy (DOE), Office of Science, Basic Energy Sciences (BES), under Award No. FG02-06ER46319. K. L. and Y. X. W. acknowledge the support of the National Natural Science Foundation of China (Grant No. 11275012). A. P. R. was supported by NSF-DMR 1534741, and J. T. was supported by NSF DGE-1339067. The work at NHMFL is supported by NSF-DMR-1157490, the State of Florida, the DOE, and additional funding from NHMFL User Collaboration.

-
- [1] A. P. Ramirez, G. P. Espinosa, and A. S. Cooper, *Phys. Rev. Lett.* **64**, 2070 (1990).
- [2] P. Lechermann, B. Bernu, C. Lhuillier, L. Pierre, and P. Sindzingre, *Phys. Rev. B* **56**, 2521 (1997).
- [3] X.-G. Wen, *Field Theory of Many-Body Systems: From the Origin of Sound to an Origin of Light and Electrons* (Oxford University Press, New York, 2007).
- [4] L. Balents, *Nature (London)* **464**, 199 (2010).
- [5] R. Schaffer, S. Bhattacharjee, and Y. B. zKim, *Phys. Rev. B* **88**, 174405 (2013).
- [6] A. S. Wills, R. Ballou, and C. Lacroix, *Phys. Rev. B* **66**, 144407 (2002).
- [7] M. Maksymenko, V. R. Chandra, and R. Moessner, *Phys. Rev. B* **91**, 184407 (2015).
- [8] Y. Zhao, W. Li, B. Xi, Z. Zhang, X. Yan, S. J. Ran, T. Liu, and G. Su, *Phys. Rev. E* **87**, 032151 (2013).
- [9] S. Sachdev, *Phys. Rev. B* **45**, 12377 (1992).
- [10] T. Picot and D. Poilblanc, *Phys. Rev. B* **91**, 064415 (2015).
- [11] P. Bordet, I. Gelard, K. Marty, A. Ibanez, J. Robert, V. Simonet, B. Canals, R. Ballou, and P. Lejay, *J. Phys. Condens. Matter* **18**, 5147 (2006).
- [12] H. D. Zhou, B. W. Vogt, J. A. Janik, Y.-J. Jo, L. Balicas, Y. Qiu, J. R. D. Copley, J. S. Gardner, and C. R. Wiebe, *Phys. Rev. Lett.* **99**, 236401 (2007).
- [13] A. Zorko, F. Bert, P. Mendels, P. Bordet, P. Lejay, and J. Robert, *Phys. Rev. Lett.* **100**, 147201 (2008).
- [14] Y. Okamoto, H. Yoshida, and Z. Hiroi, *J. Phys. Soc. Jpn.* **78**, 033701 (2009).
- [15] T. H. Han, J. S. Helton, S. Chu, D. G. Nocera, J. A. Rodriguez-Rivera, C. Broholm, and Y. S. Lee, *Nat. Phys.* **492**, 406 (2012).
- [16] S.-H. Lee, H. Kikuchi, Y. Qiu, B. Lake, Q. Huang, K. Habicht, and K. Kiefer, *Nat. Mater.* **6**, 853 (2007).
- [17] Y. Tabata, H. Kadowaki, K. Matsuhira, Z. Hiroi, N. Aso, E. Ressouche, and B. Fak, *Phys. Rev. Lett.* **97**, 257205 (2006).
- [18] J. D. M. Champion, A. S. Wills, T. Fennell, S. T. Bramwell, J. S. Gardner, and M. A. Green, *Phys. Rev. B* **64**, 140407 (2001).
- [19] A. P. Ramirez, B. S. Shastry, A. Hayashi, J. J. Krajewski, D. A. Huse, and R. J. Cava, *Phys. Rev. Lett.* **89**, 067202 (2002).
- [20] S. T. Bramwell and M. J. P. Gingras, *Science* **294**, 1495 (2001).
- [21] M. J. Harris, S. T. Bramwell, D. F. McMorrow, T. Zeiske, and K. W. Godfrey, *Phys. Rev. Lett.* **79**, 2554 (1997).
- [22] A. P. Ramirez, A. Hayashi, R. J. Cava, R. Siddharthan, and B. S. Shastry, *Nature (London)* **399**, 333 (1999).
- [23] L. Savary, K. A. Ross, B. D. Gaulin, J. P. C. Ruff, and L. Balents, *Phys. Rev. Lett.* **109**, 167201 (2012).
- [24] See Supplemental Material at <http://link.aps.org/supplemental/10.1103/PhysRevLett.116.157201>, which includes Refs. [25–27], for details of sample synthesis, measurement setups, x-ray diffraction pattern, crystallographic table with selective bond lengths, theoretical model, estimation methods for D_{nn} and J_{ex} , and magnetic entropy.
- [25] T. Sakakibara, T. Tayama, Z. Hiroi, K. Matsuhira, and S. Takagi, *Phys. Rev. Lett.* **90**, 207205 (2003).
- [26] C. Kittel, *Introduction to Solid State Physics*, 7th ed. (John Wiley and Sons, New York, 1995), p. 446.
- [27] B. Z. Malkin, T. T. A. Lummen, P. H. M. van Loosdrecht, G. Dhalenne, and A. R. Zakirov, *J. Phys. Condens. Matter* **22**, 276003 (2010).
- [28] K. Li, Y. Hu, Y. Wang, T. Kamiyama, B. Wang, Z. Li, and J. Lin, *J. Solid State Chem.* **217**, 80 (2014).
- [29] W. T. Fu and D. J. W. Ijdo, *J. Solid State Chem.* **213**, 165 (2014).
- [30] M. B. Sanders, J. W. Krizana, and R. J. Cava, *J. Mater. Chem. C* **4**, 541 (2016).
- [31] S. T. Bramwell, M. N. Field, M. J. Harris, and I. P. Parkin, *J. Phys. Condens. Matter* **12**, 483 (2000).
- [32] J. M. Luttinger and L. Tisza, *Phys. Rev.* **70**, 954 (1946).
- [33] L. Onsager, *J. Phys. Chem.* **43**, 189 (1939).
- [34] O. Nagai, S. Miyashita, and T. Horiguchi, *Phys. Rev. B* **47**, 202 (1993).
- [35] R. Siddharthan, B. S. Shastry, and A. P. Ramirez, *Phys. Rev. B* **63**, 184412 (2001).
- [36] R. Siddharthan, B. S. Shastry, A. P. Ramirez, A. Hayashi, R. J. Cava, and S. Rosenkranz, *Phys. Rev. Lett.* **83**, 1854 (1999).
- [37] R. G. Melko, B. C. den Hertog, and M. J. P. Gingras, *Phys. Rev. Lett.* **87**, 067203 (2001).
- [38] I. Mirebeau, A. Apetrei, J. Rodriguez-Carvajal, P. Bonville, A. Forget, D. Colson, V. Glazkov, J. P. Sanchez, O. Isnard, and E. Suard, *Phys. Rev. Lett.* **94**, 246402 (2005).
- [39] T. Takagi and M. Mekata, *J. Phys. Soc. Jpn.* **62**, 3943 (1993).
- [40] T. Takagi and M. Mekata, *J. Phys. Soc. Jpn.* **64**, 4609 (1995).
- [41] J. M. Kosterlitz and D. J. Thouless, *J. Phys. C* **6**, 1181 (1973).
- [42] M. A. Schmidt, D. M. Silevitch, G. Aeppli, and T. F. Rosenbaum, *Proc. Natl. Acad. Sci. U.S.A.* **111**, 3689 (2014).